Neoplasma 2022; 70(1): 71–81

doi:10.4149/neo_2022_220622N656

CBX3 promotes breast cancer progression and high level of CBX3 predicts poor prognosis in patients

Kai YANG[1,#], Ya-Lin WANG[1,#], Zhen ZHU[2,#], Xin-Hui CAO[1], Ming-Xing LIANG[2], Di XU[2], Yin-Jiao FEI[2], Si-Yuan YANG[2], Hong-Lei ZHOU[2], Jin-Hai TANG[1,2,*]

[1]Xuzhou Medical University, Xuzhou, China; [2]Department of General Surgery, The First Affiliated Hospital of Nanjing Medical University, Nanjing, China

**Correspondence: jhtang@njmu.edu.cn*
[#]Contributed equally to this work.

Received June 22, 2022 / Accepted December 12, 2022

Breast cancer is one of the leading cancer deaths around the world. Targeted drugs have greatly increased the survival rate of breast cancer patients in recent years. But in some patients, the current regimen is still ineffective. Therefore, more therapeutic targets for treating breast cancer are demanding. The core heterochromatin-related genes of breast cancer were identified by utilizing prognostic survival analysis and multivariate Cox hazard proportional regression analysis. Both breast cancer and adjacent normal tissue were collected and analyzed with western blot and immunohistochemistry. Colony formation assay, CCK-8 assay, and EdU assay were used to measure the effect of CBX3 on breast cancer cell growth, wound-healing assay and Transwell assay were used to analyze the effect of CBX3 on breast cancer cell migration and invasion. Flow cytometry assay and western blot were used to study the molecular mechanism of CBX3 in breast cancer. High expression of heterochromatin-related proteins CBX3, H2AFY, and SULF1 showed a poor prognosis in patients in both TCGA dataset and GEO datasets. Western blot demonstrated that the expression level of CBX3 was significantly higher in breast cancer than that in adjacent normal tissues. Colony formation assay, CCK-8 assay, and EdU assay showed that the knockdown of CBX3 could significantly inhibit breast cancer cell growth, and the overexpression of CBX3 could promote the growth of breast cancer cells. Transwell assay and wound healing assay showed that knockdown of CBX3 inhibited breast cancer cell migration and invasion, and the overexpression of CBX3 promoted breast cancer cell migration and invasion. Western blot showed that CBX3 might promote breast cancer cell proliferation, invasion, and migration in breast cancer by modulating the ERK1/2 signaling pathway and epithelial-mesenchymal transition (EMT)-related genes. CBX3 was a biomarker of poor prognosis in breast cancer patients. CBX3 promoted the proliferation of breast cancer cells through the ERK signaling pathway, and migration and invasion of breast cancer cells through EMT-related genes. The CBX3/p-ERK1/2 signaling axis might provide a new therapeutic method against breast cancer.

Key words: breast cancer; CBX3; TCGA; proliferation; invasion

Breast cancer (BC) is the most commonly diagnosed cancer among women and is one of the biggest public health problems worldwide [1]. The incidence of BC in the United States and other countries increased significantly in the past ten years, while the mortality rate did not increase in the same proportion, which largely benefits from progress in BC treatment. Many factors such as lifestyle and environmental factors (high-fat diet, drinking, lack of physical exercise) could increase the risk of BC [2]. Current treatments for BC include surgery, chemotherapy, radiotherapy, endocrine therapy, and targeted therapy [3]. Despite the great progress in the past, research on BC is still demanding. Especially, there is an urgent need to identify new therapeutic targets for BC.

Chromobox protein homolog 3 (CBX3) also known as Heterochromatin Protein 1 Homolog Gamma is a protein-coding gene. CBX3 plays important functions in mammalian development, cancer, aging, and tissue repair through regulating histone 3 lysine trimethylation at residues K9 (respectively, H3K9me3) [4, 5]. CBX3 participates in several molecular processes, including the silencing of gene expression [6, 7], DNA damage repair [8], and centromere cohesion protection [9]. In hepatocellular carcinoma, abnormally high expression of CBX3 is an independent prognostic factor associated with poorer disease outcomes and CBX3 overexpression promotes hepatocellular carcinoma tumorigenesis and progression [10]. Another study showed that the knock-

down of CBX3 could remarkably suppress the proliferation and colony formation ability of glioma U87 cells by blocking cell arrest at the G0/G1 phase and inducing apoptosis [11]. These studies suggested CBX3 acted as a promoter in different cancers.

But in BC, the functional roles and related mechanisms of CBX3 are not yet fully understood and await to be elucidated.

Herein, we reported that CBX3 was upregulated in BC tissues. We also found the upregulation of CBX3 was associated with poor outcomes of BC patients. In addition, we showed that CBX3 promoted proliferation, and migration/invasion in BC cell lines. Furthermore, we found CBX3 regulates the cell cycle and ERK pathway.

Patients and methods

Cell lines and chemicals. The normal breast cell (MCF-10A) and human BC cell lines (MDA-MB-231, BT-549, Hs578T) were purchased from the Cell Bank of the Chinese Academy of Sciences (Shanghai, China); human BC cells SUM1315MO2 were kindly provided by Stephen Ethier (University of Michigan, Ann Arbor, MI, USA). All cell lines were recently appraised, and we periodically evaluated cell lines for mycoplasma contamination with MycoBlue Mycoplasma Detector (Vazyme, China). The cell lines MDA-MB-231, SUM1315MO2, Hs578T were cultured in Dulbecco's modified Eagle's medium (DMEM) high glucose (KeyGEN, China), supplemented with 10% fetal bovine serum (FBS) (Wisent, China), and BT-549 cells were cultured in DMEM with 20% FBS, and all cell lines were cultures in 1% penicillin/streptomycin. All cells were incubated at 37 °C with 5% CO_2.

Transfection, plasmid construction, and lentivirus infection. CBX3 siRNA sequences were provided by RIBOBIO (Guangzhou China). Three selected siRNA targeting CBX3 were used to filter out a stronger knockdown sequence, including siRNA sequence 1 (GGAGAATTGATGTTTCTCA); siRNA sequence 2 (GAAGTGTCCTCAAATTGTA); siRNA sequence 3 (TCTTGATCCTGAAAGAATA). siRNA sequence 2 produced a stronger knockdown effect compared to siRNA sequence 1 and sequence 3; therefore, sequence 2 was used in our subsequent experiments. Cells were transfected with siRNA using Lipofectamine 8000 reagent (Beyotime, China) according to the manufacturer's instructions.

CBX3 overexpression, ectopic expression viral particles were generated from 293T cells, followed by the transduction of BT-549 and Hs578T cells, respectively. Cells were selected with 2 μg/ml puromycin (P8833, Sigma-Aldrich, St. Louis, MO, USA) or 2 μg/ml blasticidin S (BSD, SBR00022, Sigma-Aldrich) for 5 days.

Bioinformatics analysis. Gene expression and parallel clinical data of GSE70951, GSE134359, and GSE14999 were downloaded from Gene Expression Omnibus (GEO) databases. For the multiple probes, the mean expression was used. Gene expression and clinical data of The Cancer Genome Atlas Breast Cancer (TCGA-BRCA) were retrieved from Genomic Data Commons Data Portal. Differently expressed genes in normal and tumor specimens were generated with Limma (R-package) with a statistical difference (LogFC >1, FDR <0.05). The survival analysis was performed with online Kaplan-Meier Plotter. The clinicopathologic information was analyzed with the 'forestplot' package.

Clinical samples. Fifteen pairs of fresh BC tissues and adjacent non-tumorous tissues were acquired from the patients from Jiangsu Provincial People's Hospital. The informed consent form was signed by all patients and the research protocol was officially approved by the ethics committees of the Jiangsu Provincial People's Hospital (2021-SR-499).

RNA isolation and real-time quantitative PCR (RT-qPCR). The total RNA of cultured cells was isolated by TRIzol reagent (Thermo Fisher Scientific, USA). HiScript II Q RT SuperMix for qPCR (Vazyme) was used to reverse transcribe RNA into cDNA. The procedure of PCR was conducted by the method of ChamQ SYBR qPCR Master Mix (High ROX Premixed) (Vazyme) on the StepOnePlus Real-Time PCR System (Thermo Fisher Scientific, USA). The expression of target genes was calculated based on the cycle threshold (Ct) values compared with GAPDH using the $2^{-\Delta\Delta Ct}$ method. The primer sequences were as follows: GAPDH forward primers: 5'-GGAGCGAGATCCCTCCAAAAT-3'; reverse primers: 5'-GGCTGTTGTCATACTTCTCATGG-3'; CBX3 forward primers: 5'-TAGATCGACGTGTAGTGAATGGG-3'; reverse primers: 5'-TGTCTGTGGCACCAATTATTCTT-3'.

Western blotting. Total protein from tissues or cells was extracted by the RIPA buffer containing phosphatase and protease inhibitor. The protein was quantified by a BCA protein determination kit (Beyotime). Subsequently, SDS-PAGE was used to separate the proteins and then proteins were transferred onto a polyvinylidene fluoride (PVDF) membrane. Then the membrane was blocked with Quickblock western (Beyotime) and incubated with primary antibodies at 4 °C overnight. After washing in TBST three times, the membranes were incubated with horseradish peroxidase (HRP)-conjugated anti-rabbit or anti-mouse antibodies for 1 h at room temperature. The western blots were visualized with an ECL substrate kit (Tanon Science and Technology, Shanghai, China). The antibodies used are listed in Supplementary Table S1.

Cell proliferation assay. The experimental and control group cells were inoculated in a 96-well plate at 2000 cells/well. Based on the manufacturer's instructions, 10 μl of CCK-8 working buffer was added into 100 μl medium in each well for 2 h, then the optical density (OD) was measured by a Multiskan FC spectrophotometer (Thermo Fisher Scientific, USA) at a wavelength of 450 nm. The value we measured after the cells were seeded on the 96-well plate 24 was recorded as

0 h. Subsequently, the OD value of 0, 24, 48, and 72 hours was measured in the same way.

5-ethynyl-2'-deoxyuridine (EdU) assay. According to the manufacturer's (RiboBio, China) instruction, cells were exposed to 50 μM EdU for two hours at 37 °C, then the cells were fixed in 4% paraformaldehyde. After permeabilization with 0.5% Triton-X, the cells were incubated with 1× Apollo reaction cocktail (RiboBio) for 30 min. Then, the DNA contents of the cells in each well were stained with DAPI for 30 min and visualized under a fluorescence microscope.

Colony formation assay. About 800 cells were seeded in 6-well plates in a medium with 10% FBS. The cells were incubated immovably with 5% CO_2 at 37 °C for 10–15 days until control cells formed colonies. Next, the cells were fixed with 4% paraformaldehyde for 40 min and soaked with 1% crystal violet for 1 h. ImageJ software (NIH, USA) was used for quantifying the colony numbers (colonies with >50 cells).

Cell cycle assay. The MDA-MB-231 and SUM1315MO cells were seeded in a 6-well plate at 3×10^5 cells/well. After 24 h, cells were transfected with CBX3 siRNA or control siRNA, and then cultured for 48 h. The cells were then collected and counted. 1.0×10^6 cells/sample were used for flow cytometry analysis. The cells were first rinsed with cold phosphate-buffered saline (PBS) prior to an overnight fixation with 70% ethanol at 4 °C. The next day, staining buffer (PBS containing 1 mg/ml PI and 10 mg/ml RNase A) was used to treat the cells for 30 min in a dark room at 37 °C. Then the stained cells were analyzed with flow cytometry (Beckman Coulter, USA) and the results were analyzed with WinCycle software (Phoenix Flow Systems, San Diego, CA, USA).

Wound-healing assay. Transfected cells were seeded at 4×10^5 cells/well onto a 6-well dish and incubated until they reached more than 90% confluence. Scratches were made by a sterile 200 μl pipette tip and washed twice with PBS to remove the floating cells. The FBS-free medium was added and cultured for 48 h, and photographs were taken by a fluorescence microscope at 0 and 48 h. The cell migration rate of each group was calculated based on a relative of wound closure.

Immunohistochemistry. According to the kit instructions of Maxim China, about 68 breast cancer tissues and 14 normal breast tissues were used for staining with CBX3 antibody. The related expression levels were scored as the intensity of the staining (0 = no staining; 1 = weak staining; 2 = moderate staining; 3 = intense staining). The antibodies used are listed in Supplementary Table S1.

Transwell assay. Transwell assay was performed using Corning Transwell Kit. About 1×10^6 cells were incubated in the upper chamber with 100 μl medium without FBS in a 24-well plate and 500 μl medium supplemented with 10% FBS was added in the lower chamber. Cells were cultured for 48 h and stained with 4% formaldehyde, soaked with 1% crystal violet. Lastly, the migration ability of cells was analyzed.

Statistical analysis. Statistical analysis was performed using GraphPad Prism version 8.0.2 for Windows. All experiments were independently iterated three times. The unpaired Student's t-test was used for the two experimental groups while one-way analysis of variance (ANOVA) followed by Dunnett's or Bonferroni's multiple comparison test for datasets from multiple experimental groups. Data were accepted when $p<0.05$.

Results

CBX3 expression was associated with BC prognosis. We analyzed the differentially expressed genes in TCGA BRCA dataset and three microarray datasets GSE14999, GSE70951, and GSE134359 from the GEO database with the Sangerbox software v1.0.8. We first identified 57 differentially expressed heterochromatin genes from these four BC datasets by using Venn diagrams (Figure 1A). Then we utilized the heatmap to visualize these 57 heterochromatins in GSE14999 (Figure 1B). The other three heatmaps of TCGA, GSE70951, and GSE134359 are presented in Supplementary Figure S1. We screened 12 genes associated with BC survival prognosis based on the online website (http://kmplot.com/) (Figure 1C, Supplementary Figure S2). Then, by analyzing the correlation between gene expressions and clinical traits of BC, we screened out three hub genes CBX3, H2AFY, and SULF1 (Figures 1D, 1E, Supplementary Figure S3). As shown in Figures 1D and 1E, low expression of CBX3 predicts a better prognosis (Figures 1D, 1E). Detailed differentially expressed genetic information is listed in Supplementary Table S2.

CBX3 expression was upregulated in BC. CBX3 was highly expressed in BC compared to normal breast tissue based on datasets from TCGA, GSE14999, GSE70951, and GSE134359 (Figure 2A). To confirm the above results, we collected 15 pairs of tissue samples from BC patients and analyzed their CBX3 expression levels with western blot (Figure 2B). The results showed that CBX3 expression was upregulated in BC. IHC results of 82 BC patients' samples showed CBX3 was in the nucleus and the expression level in BC was higher than that in normal breast tissue (Figure 2C). In addition, we analyzed both mRNA and protein expression levels of CBX3 in BC cell lines. The results showed that CBX3 expression was upregulated in most BC cell lines compared to normal mammary epithelial cell MCF-10A (Figures 2D, 2E).

Knockdown of CBX3 suppressed BC cells' proliferation. The upregulation of CBX3 in BC tissues suggested that CBX3 might function as a tumor promoter. To confirm this hypothesis, we first studied the effects of CBX3 on cell proliferation. The MDA-MB-231 and SUM1315MO cells were transfected with CBX3 siRNA. Both mRNA and protein levels of CBX3 were inhibited as shown in (Figures 3A, 3B). EdU and colony formation assays showed that the knockdown of CBX3 effectively suppressed the proliferation of both MDA-MB-231 and SUM1315MO cells (Figures 3C, 3D). Moreover, the CCK-8 assay result indicated that MDA-MB-231 and SUM1315MO cells with low CBX3 expression had a sluggish growth rate compared to the control group at 48 h and 72 h (Figure 3E).

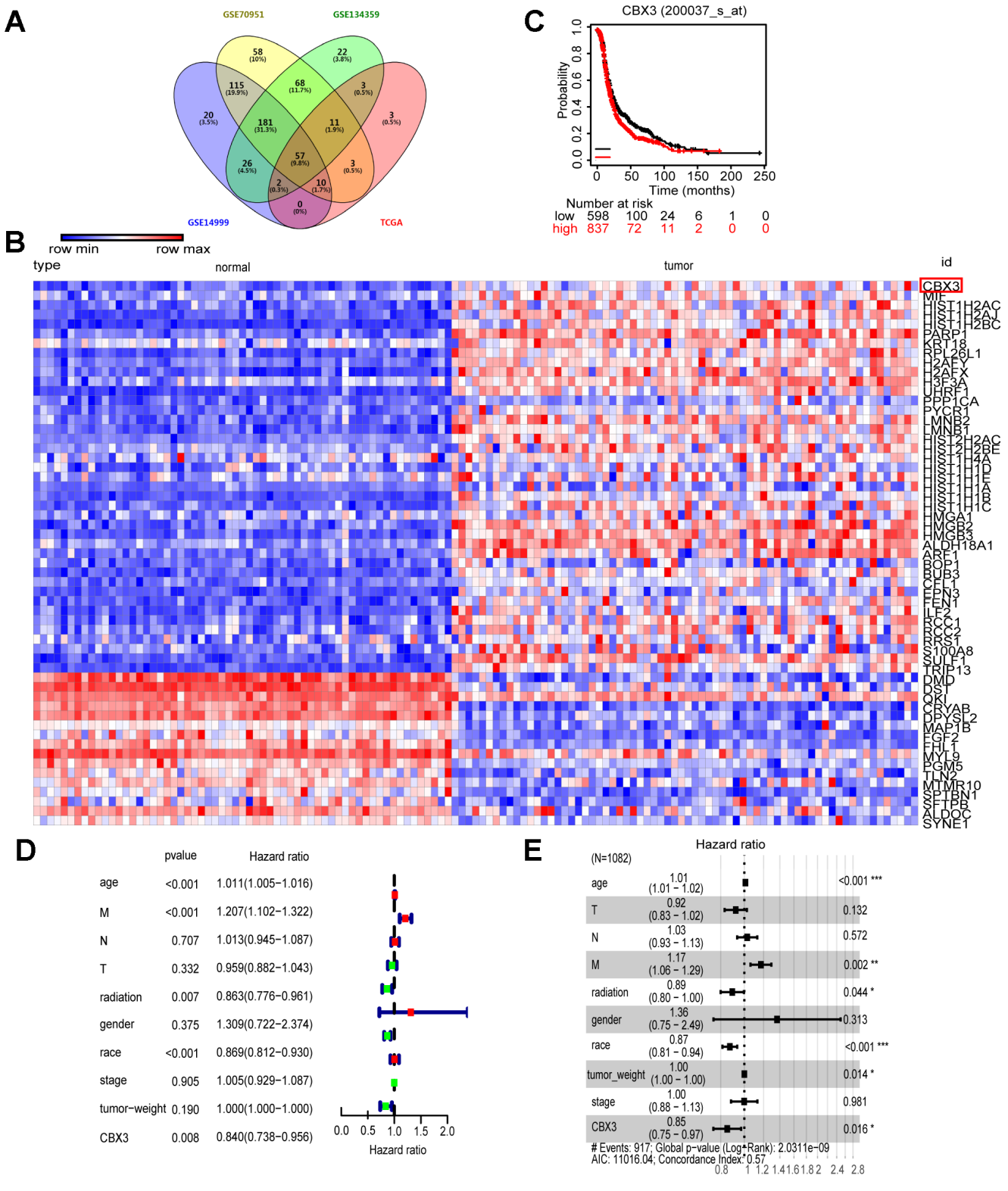

Figure 1. CBX3 was associated with BC prognosis. A) Differentially expressed heterochromatin genes in TCGA and GEO BC datasets. B) Heatmaps of 57 heterochromatin genes in GSE14999. C) KM-plot showed high expression of CBX3 correlated with poor prognosis in BC. D, E) Univariate and multivariate Cox analysis of TCGA BRCA clinical database.

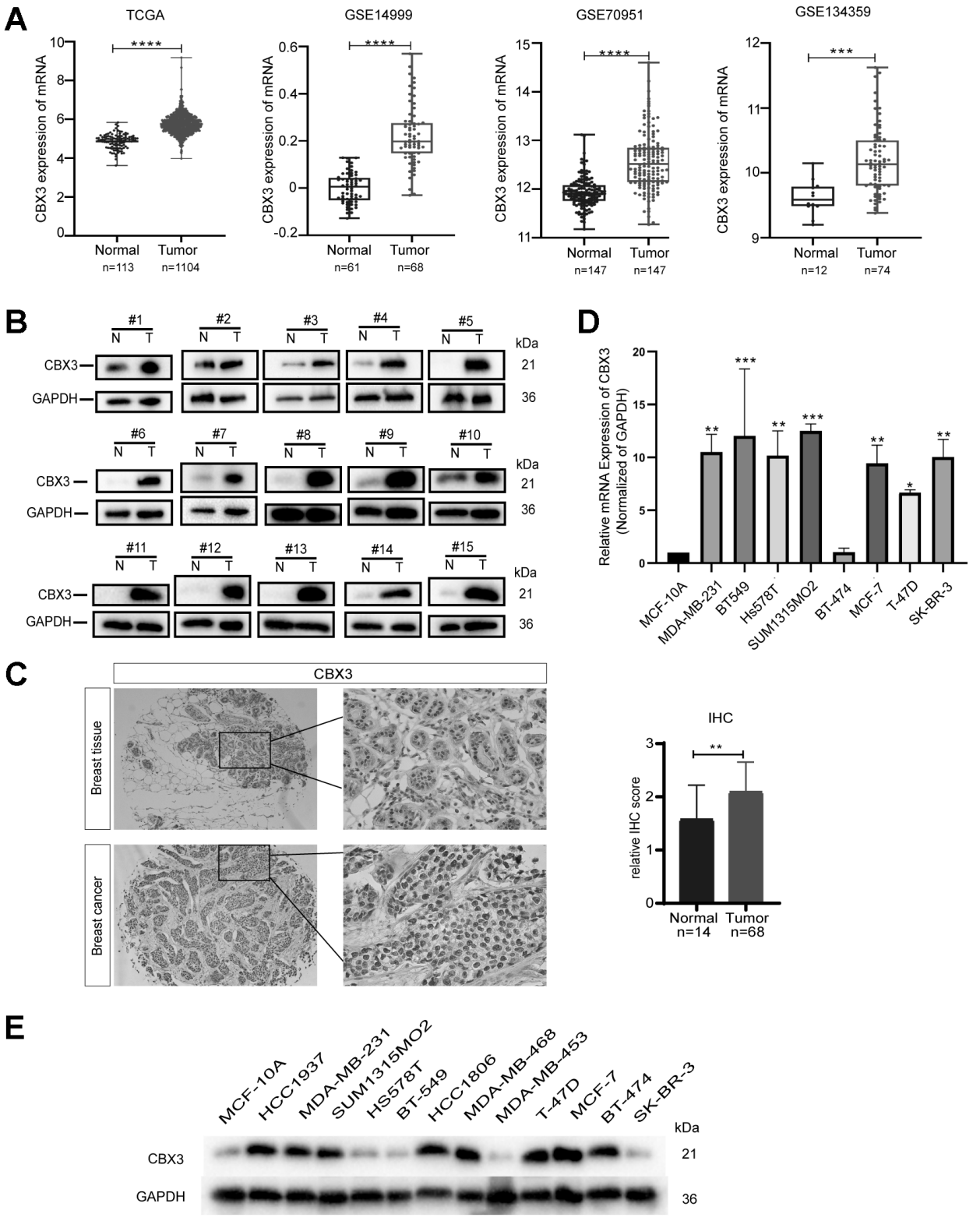

Figure 2. CBX3 expression was upregulated in BC. A) CBX3 mRNA was upregulated in TCGA and GEO datasets. B) CBX3 protein expression was upregulated in BC tissues (T) compared to adjacent normal tissues (N). C) IHC staining of CBX3 in BC and breast tissues. D) CBX3 mRNA expression in BC cell lines. E) CBX3 protein expression in BC cell lines.

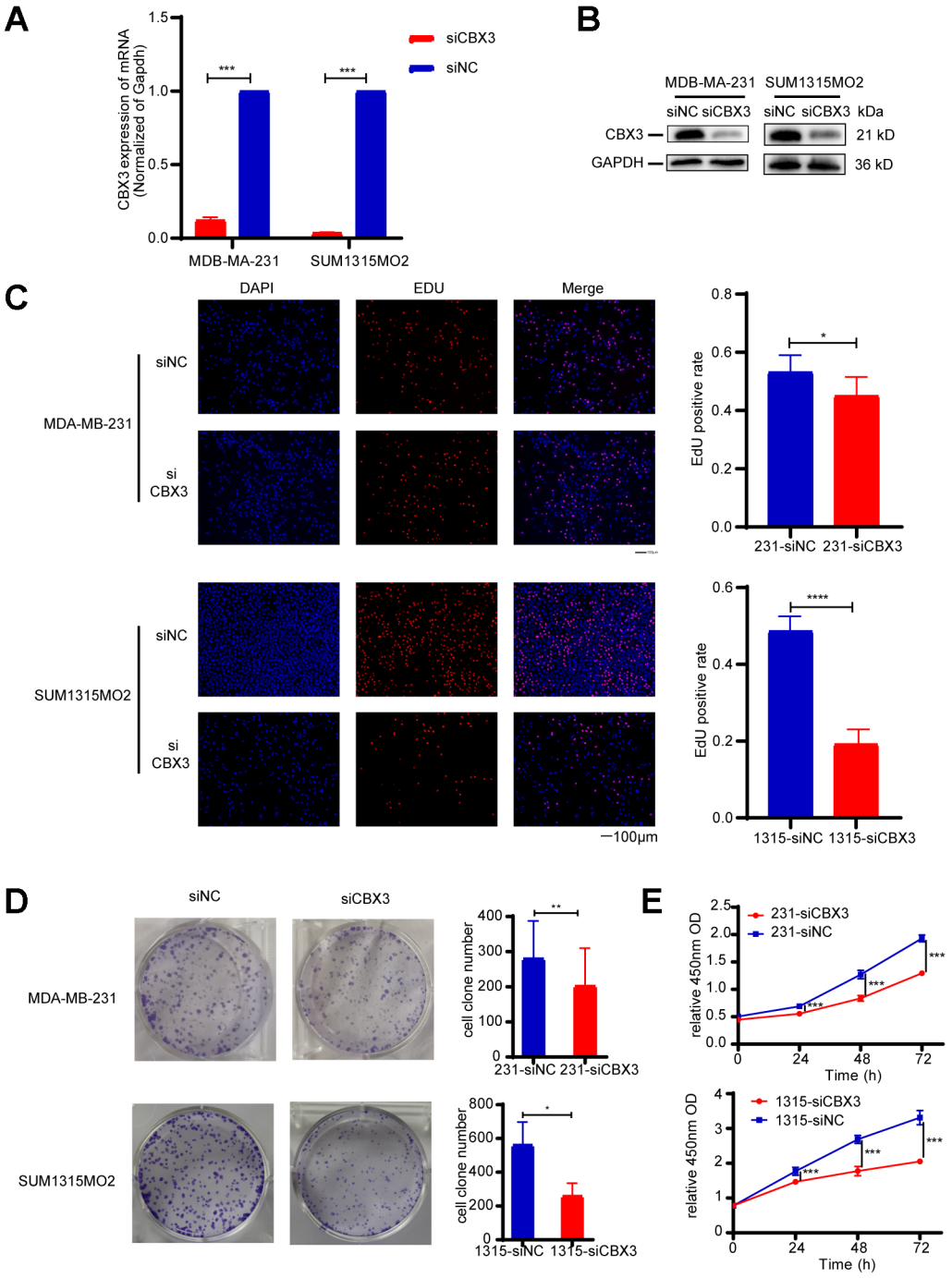

Figure 3. Knockdown of CBX3 suppressed BC cells' proliferation. A, B) The efficiency of CBX3 silence in mRNA and protein expression levels. C) EdU assay, D) colony formation assay, E) CCK-8 assay showed knockdown of CBX3 inhibited BC cells' proliferation.

Overexpression of CBX3 promoted BC cells' proliferation. To further confirm the effect of CBX3 on BC cell proliferation, we overexpressed CBX3 by lentiviral transduction in BT-549 and Hs578T cells, which had low endogenous CBX3 expression. The transduced cells were selected with blasticidin. Western blot showed both BT-549 and Hs578T cell lines stably overexpressing CBX3 (Figure 4A). EdU assay showed that the overexpression of CBX3 in BT-549 and Hs578T cells promoted cell proliferation (Figure 4B). CCK-8 assay also proved that BT-549 and Hs578T cells with CBX3 overexpression had a higher growth rate compared to the parental cells after 48 h, 72 h, and 96 h (Figure 4C).

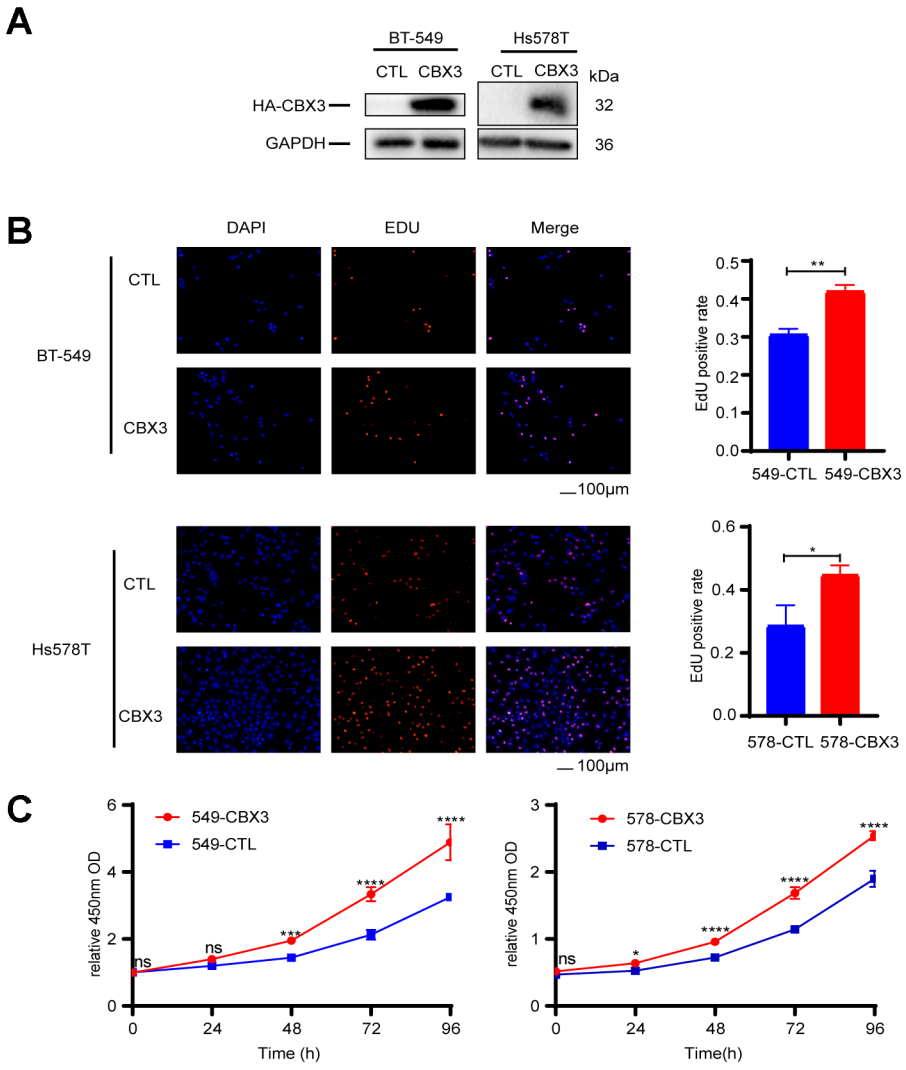

Figure 4. Overexpression of CBX3 promoted BC cells' proliferation. A) CBX3 protein levels in CBX3-overexpressed stable cell lines and respective control cell lines. B) EdU assay, C) CCK-8 assay indicated that the overexpression CBX3 stimulated BC cells' progression.

CBX3 promoted BC cells' migration and invasion via regulating epithelial-mesenchymal transition (EMT)-related proteins. Our multivariate Cox analysis above demonstrated that metastasis was also related to BC long-term survival. To investigate whether CBX3 might be involved in the migration of BC cells, Transwell and wound-healing assays were conducted. Transwell assay showed that the knockdown of CBX3 in MDA-MB-231 cells significantly suppressed the migration capabilities, while the overexpression of CBX3 in BT-549 cells markedly enhanced migration compared to the negative control group (Figures 5A, 5C). The wound-healing assay showed the same trends as the Transwell assay (Figures 5B, 5D). As cell migration is related to the EMT process, we then studied the molecular effects of CBX3 knockdown/overexpression on EMT-related proteins such as ZEB1, E-cadherin, N-cadherin, and Vimentin by using western blot. Our results showed that the overexpression of CBX3 in BT549 cells induced N-cadherin, Vimentin, and ZEB1 expression while suppressing E-cadherin expression (Figure 5F). Treatment of CBX3-overexpressed cells with 10 μM metformin reduced both N-cadherin and Vimentin expression and induced E-cadherin expression (Supplementary Figure S4A), thus reducing the cell invasion (Supplementary Figure S4B). Knockdown of CBX3 in MDA-MB-231 cells suppressed Vimentin and ZEB1 expression while inducing E-cadherin expression (Figure 5E). We did not detect N-cadherin expression in MDA-MB-231 cells. These results indicated that CBX3 might promote BC cells' migration by regulating EMT-related genes.

CBX3 regulated the cell cycle and activated the ERK pathway. Previous studies showed CBX3 promoted cancer

cell proliferation by regulating the cell cycle. To test whether CBX3 regulated cell cycle transition, we knocked down CBX3 in MDA-MB-231 and SUM1315MO2 cell lines and used flow cytometry to check the cell cycle. As shown in Figures 6A and 6B, the knockdown of CBX3 resulted in a halt of the cell cycle at the S phase. Western blot result showed that the knockdown of CBX3 inhibited CDC2 expression in both cell lines but there was no change in cyclin D1 and p27 expression (Figure 6C). As the MAPK/ERK kinase, STAT3, and PI3K/AKT pathways play important roles in the proliferation and metastasis of multiple cancers, we also studied the effect of CBX3 on these signaling pathways. As shown in Figure 6D, the knockdown of CBX3 inhibited ERK phosphorylation in both MDA-MB-231 and SUM1315MO2 cells, and overexpression of CBX3 promoted ERK phosphorylation in both BT-549 and Hs578T cells. Treatment of CBX3-overexpressed Hs578T cells with ERK1/2 inhibitor (SCH772984) reduced ERK1/2 phosphorylation compared to the CBX3-overexpressed Hs578T cells treated with DMSO (Supplementary Figure S4C). Meanwhile, the growth rate of CBX3-overexpressed Hs578T cells reduced after SCH772984 treatment (Supplementary Figure S4D). AKT phosphorylation was inhibited in SUM1315MO2 cells when CBX3 was knocked down, and promoted in both BT-549 and Hs578T cells when CBX3 was overexpressed. These results suggested that CBX3 promoted the proliferation, invasion, and migration of BC cells by upregulating the p-ERK1/2 level generally and p-AKT in some cells.

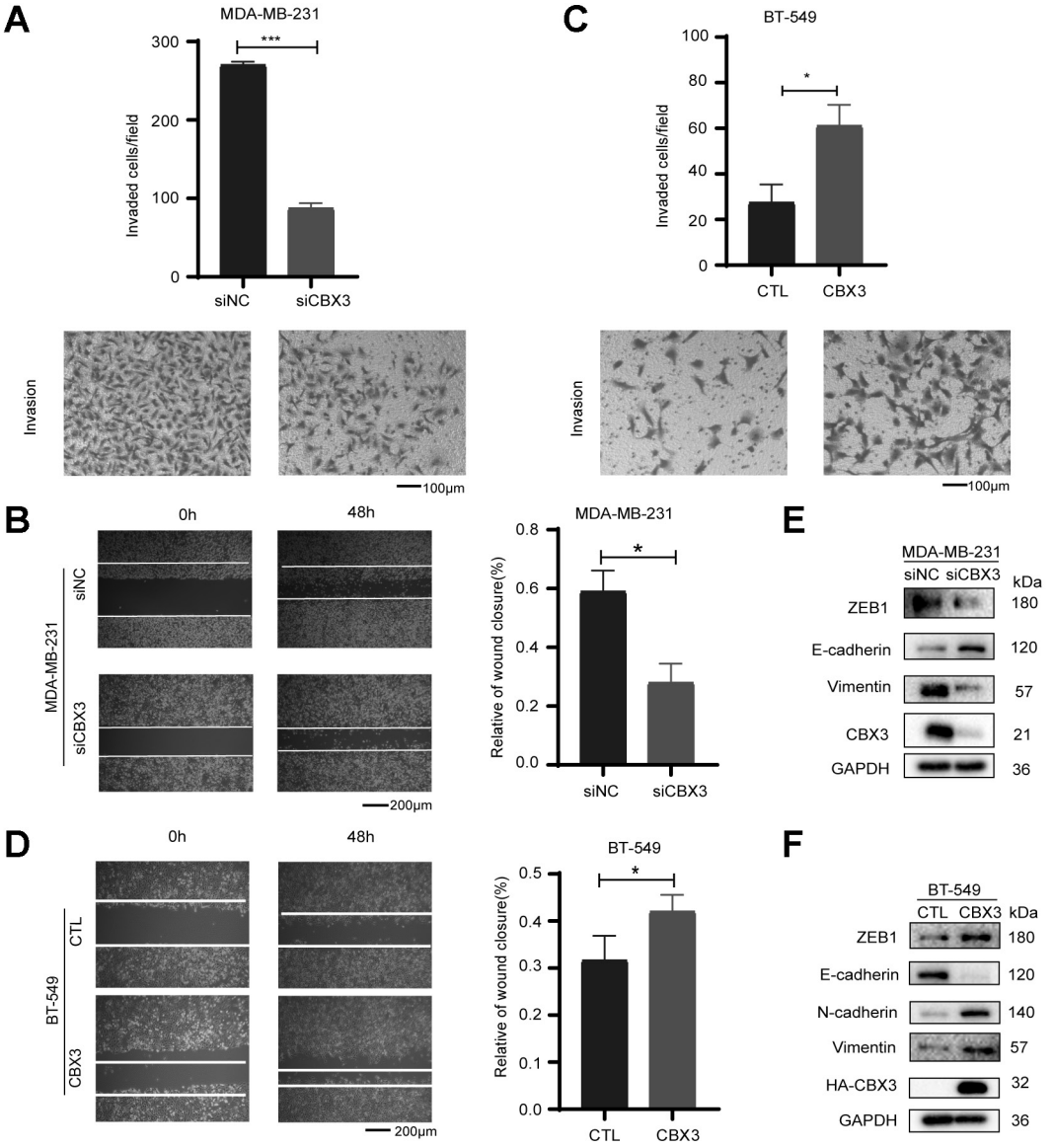

Figure 5. CBX3 promoted BC cells' invasion and migration. Effects of CBX3 knockdown on cell invasion (A) and migration (B). Effects of CBX3 overexpression on cell invasion (C) and migration (D). E, F) Epithelial and mesenchymal transition markers were detected by western blot.

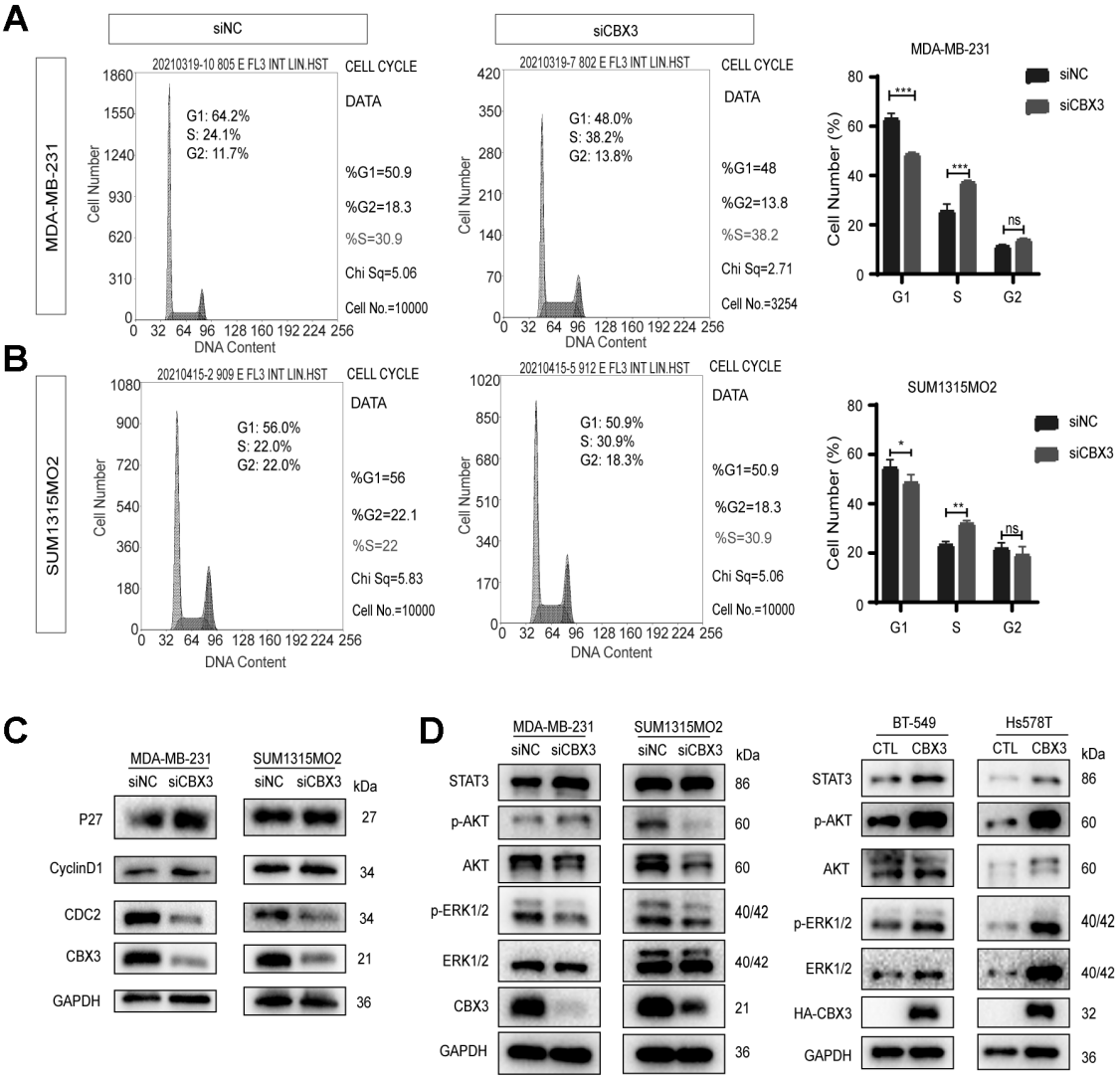

Figure 6. CBX3 regulated the cell cycle and activated the ERK pathway. A, B) CBX3 knockdown blocked the cell cycle at the S phase. C) Cyclin molecules were detected via western blot. D) Western blot showed ERK, p-ERK, AKT, p-AKT, and STAT3 levels in different cell lines after the knockdown of CBX3.

Discussion

Chromatin is a linear composite structure containing DNA, histone proteins, non-histone proteins, and a few RNA. Based on morphological characteristics, activity state, and chromatin properties, it is divided into two types: euchromatin and heterochromatin. Euchromatin has been extensively studied due to its high transcriptional activity and efficient delivery of genetic material. But more researchers realized that changes in heterochromatin composition were also related to tumorigenesis and cancer progression [12, 13].

In this study, we identified 57 heterochromatin-associated proteins aberrantly expressed in BC by intersecting differentially expressed genes (TCGA, GSE14999, GSE70951, GSE134359) with heterochromatin-associated proteins [14]. Further analysis showed that CBX3, SULF1, and H2AFY were associated with survival, prognosis, and clinical characteristics in BC. Functions of SULF1 and H2AFY in BC had been reported in previous studies [15, 16], while the role of CBX3 in BC was not well elaborated. Here we found that CBX3 was overexpressed in BC and functional studies confirmed that dysregulation of CBX3 accelerates the development and progression of BC by activating the ERK signal and regulating cyclin CDC2.

Consistent with previous studies, we confirmed CBX3 as a promoter in tumorigenesis and development. MAPK/ERK signaling pathway is an evolutionarily conservative signaling

pathway that regulates a variety of cellular processes, including cell survival, proliferation, and differentiation [17–19]. In addition, abnormal activation of this pathway promotes cancer progression in multiple cancers such as colon cancer [20], hepatocellular carcinoma [21], and prostate cancer [22]. In this study, knockdown of CBX3 expression level directly reduced the ERK1/2 phosphorylation level and overexpression of CBX3 significantly increased ERK1/2 phosphorylation, although there was no consistent change in ERK1/2 expression, suggesting that CBX3 regulating ERK activating instead of ERK expression. However, how CBX3 induces ERK1/2 phosphorylation is still unknown. Further studies are required.

In summary, our data demonstrated that CBX3 acted as a tumor promoter in BC, which could promote cell proliferation and migration. CBX3 promoted cell migration by upregulating EMT-related proteins and enhanced cell proliferation by activating the ERK pathway. This newly identified CBX3 as an oncogene in BC may provide new therapeutic strategies against BC.

Supplementary information is available in the online version of the paper.

Acknowledgments: This research was supported by the National Natural Science Foundation of China (NO.81902987 and 82102780) and High-level Innovative and Entrepreneurial Talent Introduction Plan of Jiangsu Province (303073540ER21).

References

[1] BAADE P. Geographical Variation in Breast Cancer Outcomes. Int J Environ Res Public Health 2017; 14: 523. https://doi.org/10.3390/ijerph14050523

[2] KOLAK A, KAMIŃSKA M, SYGIT K, BUDNY A, SURDYKA D et al.Primary and secondary prevention of breast cancer. Ann Agric Environ Med 2017; 24: 549–553. https://doi.org/10.26444/aaem/75943

[3] WAKS AG, WINER EP. Breast Cancer Treatment: A Review. JAMA 2019; 321: 288–300. https://doi.org/10.1001/jama.2018.19323

[4] VAN WIJNEN AJ, BAGHERI L, BADRELDIN AA, LARSON AN, DUDAKOVIC A et al. Biological functions of chromobox (CBX) proteins in stem cell self-renewal, lineage-commitment, cancer and development. Bone 2021; 143: 115659. https://doi.org/10.1016/j.bone.2020.115659

[5] MATHISON A, MILECH DE ASSUNCAO T, DSOUZA NR, WILLIAMS M, ZIMMERMANN MT et al. Discovery, expression, cellular localization, and molecular properties of a novel, alternative spliced HP1γ isoform, lacking the chromoshadow domain. PLoS One 2020; 15: e0217452. https://doi.org/10.1371/journal.pone.0217452

[6] CANZIO D, LARSON A, NARLIKAR GJ. Mechanisms of functional promiscuity by HP1 proteins. Trends Cell Biol 2014; 24: 377–386. https://doi.org/10.1016/j.tcb.2014.01.002

[7] SMALLWOOD A, HON GC, JIN F, HENRY RE, ESPINOSA JM et al. CBX3 regulates efficient RNA processing genome-wide. Genome Res 2012; 22: 1426–1436. https://doi.org/10.1101/gr.124818.111

[8] BALL AR JR, YOKOMORI K. Revisiting the role of heterochromatin protein 1 in DNA repair. J Cell Biol 2009; 185: 573–575. https://doi.org/10.1083/jcb.200904033

[9] YI Q, CHEN Q, LIANG C, YAN H, ZHANG Z et al. HP1 links centromeric heterochromatin to centromere cohesion in mammals. EMBO Rep 2018; 19: e45484. https://doi.org/10.15252/embr.201745484

[10] ZHONG X, KAN A, ZHANG W, ZHOU J, ZHANG H et al. CBX3/HP1γ promotes tumor proliferation and predicts poor survival in hepatocellular carcinoma. Aging (Albany NY) 2019; 11: 5483–5497. https://doi.org/10.18632/aging.102132

[11] ZHAO SP, WANG F, YANG M, WANG XY, JIN CL et al. CBX3 promotes glioma U87 cell proliferation and predicts an unfavorable prognosis. J Neurooncol 2019; 145: 35–48. https://doi.org/10.1007/s11060-019-03286-w

[12] FEINBERG AP, KOLDOBSKIY MA, GÖNDÖR A. Epigenetic modulators, modifiers and mediators in cancer aetiology and progression. Nat Rev Genet 2016; 17: 284–299. https://doi.org/10.1038/nrg.2016.13

[13] JOHANSEN S, GJERSTORFF MF. Interaction between Polycomb and SSX Proteins in Pericentromeric Heterochromatin Function and Its Implication in Cancer. Cells 2020; 9: 226. https://doi.org/10.3390/cells9010226

[14] BECKER JS, MCCARTHY RL, SIDOLI S, DONAHUE G, KAEDING KE et al.Genomic and Proteomic Resolution of Heterochromatin and Its Restriction of Alternate Fate Genes. Mol Cell 2017; 68: 1023–1037.e1015. https://doi.org/10.1016/j.molcel.2017.11.030

[15] CHEN F, ZHANG Z, YU Y, LIU Q, PU F. HSulf-1 and palbociclib exert synergistic antitumor effects on RB-positive triple-negative breast cancer. Int J Oncol 2020; 57: 223–236. https://doi.org/10.3892/ijo.2020.5057

[16] HALVORSEN AR, HELLAND A, FLEISCHER T, HAUG KM, GRENAKER ALNAES GI et al. Differential DNA methylation analysis of breast cancer reveals the impact of immune signaling in radiation therapy. Int J Cancer 2014; 135: 2085–2095. https://doi.org/10.1002/ijc.28862

[17] DEGIRMENCI U, WANG M, HU J. Targeting Aberrant RAS/RAF/MEK/ERK Signaling for Cancer Therapy. Cells 2020; 9: 198. https://doi.org/10.3390/cells9010198

[18] BARBOSA R, ACEVEDO LA, MARMORSTEIN R. The MEK/ERK Network as a Therapeutic Target in Human Cancer. Mol Cancer Res 2021; 19: 361–374. https://doi.org/10.1158/1541-7786.mcr-20-0687

[19] XIE JW, HUANG XB, CHEN QY, MA YB, ZHAO YJ et al. m(6)A modification-mediated BATF2 acts as a tumor suppressor in gastric cancer through inhibition of ERK signaling. Mol Cancer 2020; 19: 114. https://doi.org/10.1186/s12943-020-01223-4

[20] UROSEVIC J, BLASCO MT, LLORENTE A, BELLMUNT A, BERENGUER-LLERGO A et al. ERK1/2 Signaling Induces Upregulation of ANGPT2 and CXCR4 to Mediate Liver Metastasis in Colon Cancer. Cancer Res 2020; 80: 4668–4680. https://doi.org/10.1158/0008-5472.can-19-4028

[21] NG KY, CHAN LH, CHAI S, TONG M, GUAN XY et al. TP53INP1 Downregulation Activates a p73-Dependent DUSP10/ERK Signaling Pathway to Promote Metastasis of Hepatocellular Carcinoma. Cancer Res 2017; 77: 4602–4612. https://doi.org/10.1158/0008-5472.can-16-3456

[22] XU CJ, DONG LL, KANG XL, LI ZM, ZHANG HY. Leptin promotes proliferation and inhibits apoptosis of prostate cancer cells by regulating ERK1/2 signaling pathway. Eur Rev Med Pharmacol Sci 2020; 24: 8341–8348. https://doi.org/10.26355/eurrev_202008_22630

https://doi.org/10.4149/neo_2022_220622N656

CBX3 promotes breast cancer progression and high level of CBX3 predicts poor prognosis in patients

Kai YANG[1,#], Ya-Lin WANG[1,#], Zhen ZHU[2,#], Xin-Hui CAO[1], Ming-Xing LIANG[2], Di XU[2], Yin-Jiao FEI[2], Si-Yuan YANG[2], Hong-Lei ZHOU[2], Jin-Hai TANG[1,2,*]

Supplementary Information

Supplementary Tables are available in the online version as Excel files.

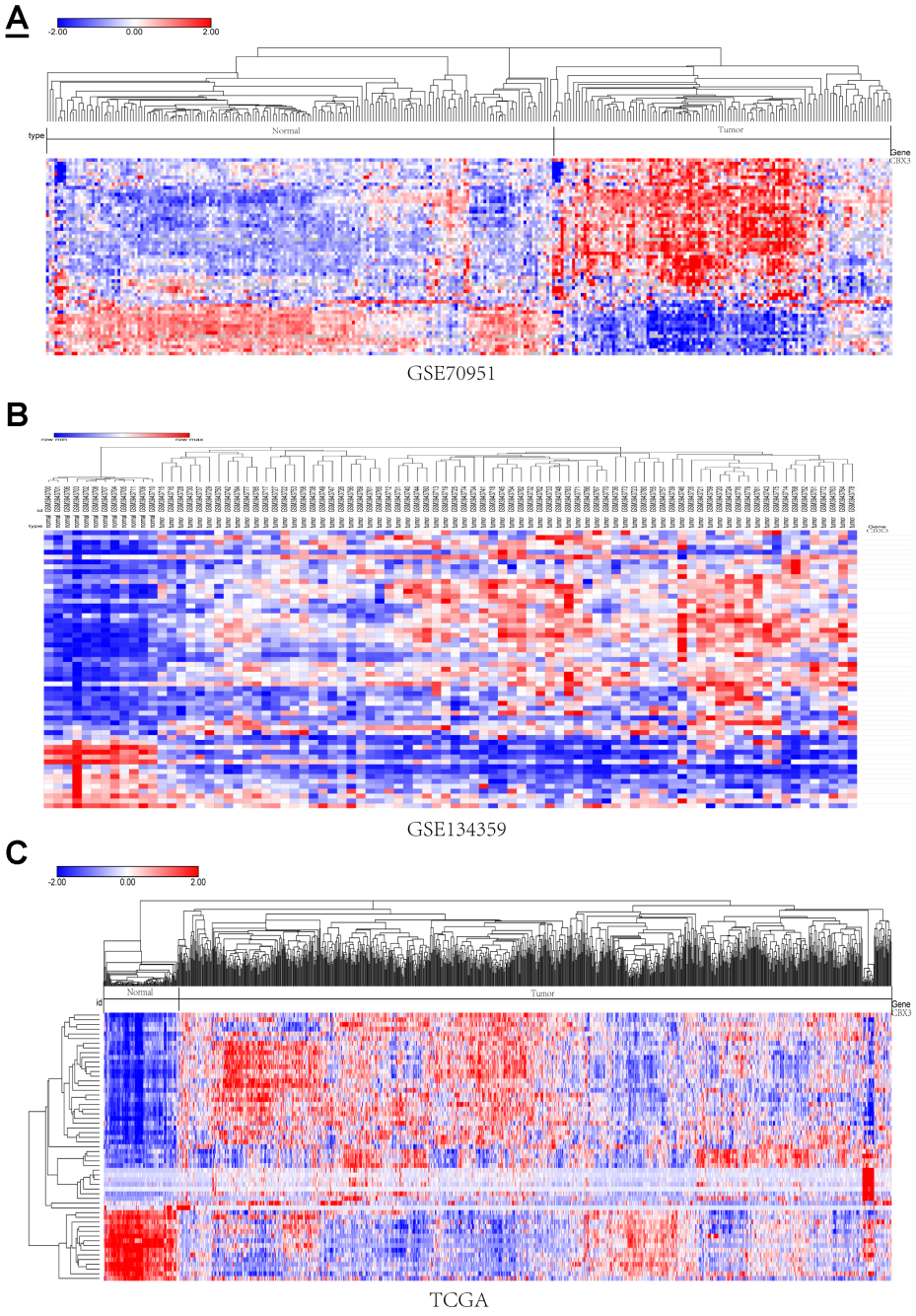

Supplementary Figure S1: Heatmap plot showed heterochromatin genes expression in datasets: A) GSE70951, B) GSE134359 and C) TCGA.

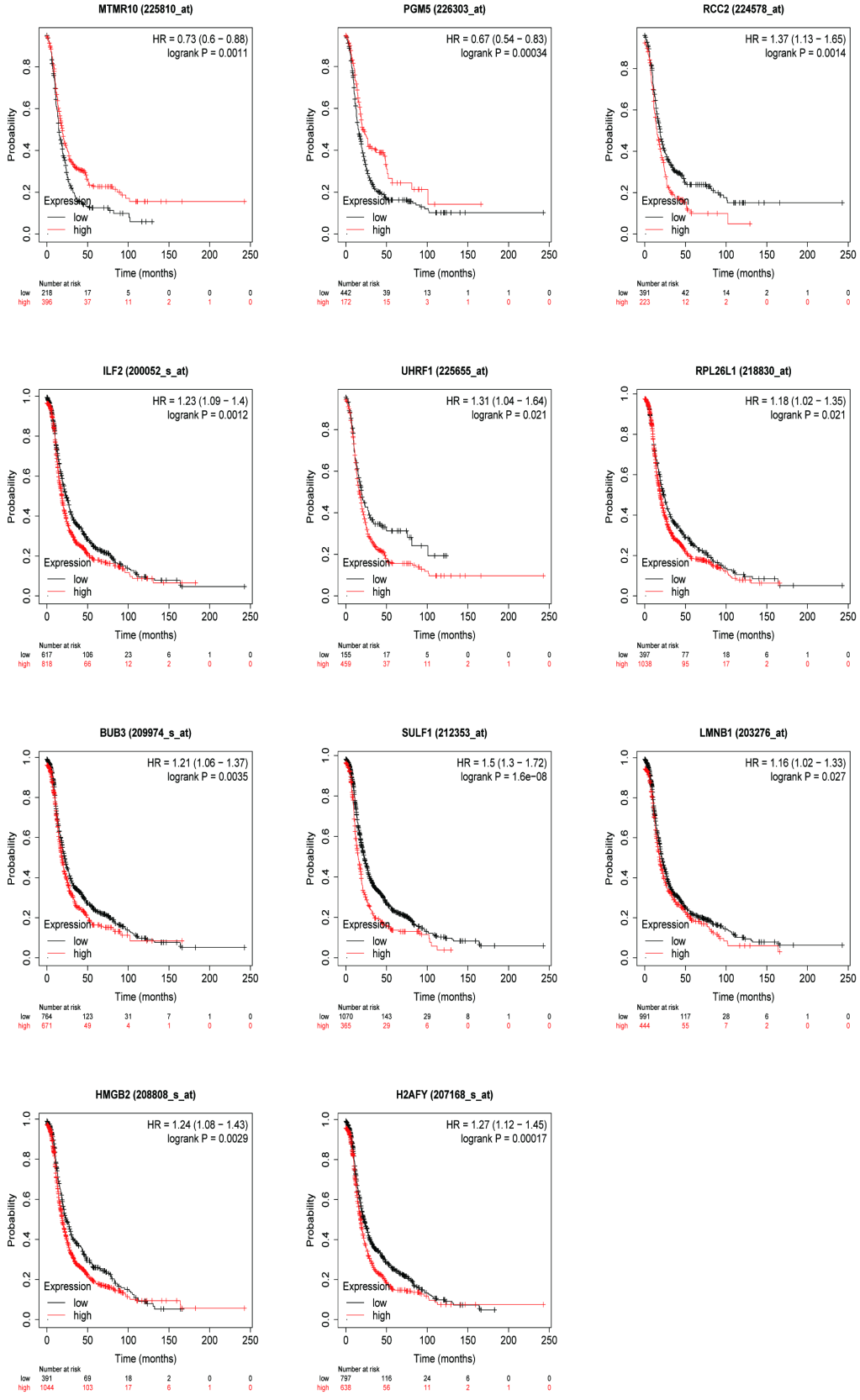

Supplementary Figure S2: KM-plot showed other 11 genes were associated with breast cancer survival prognosis.

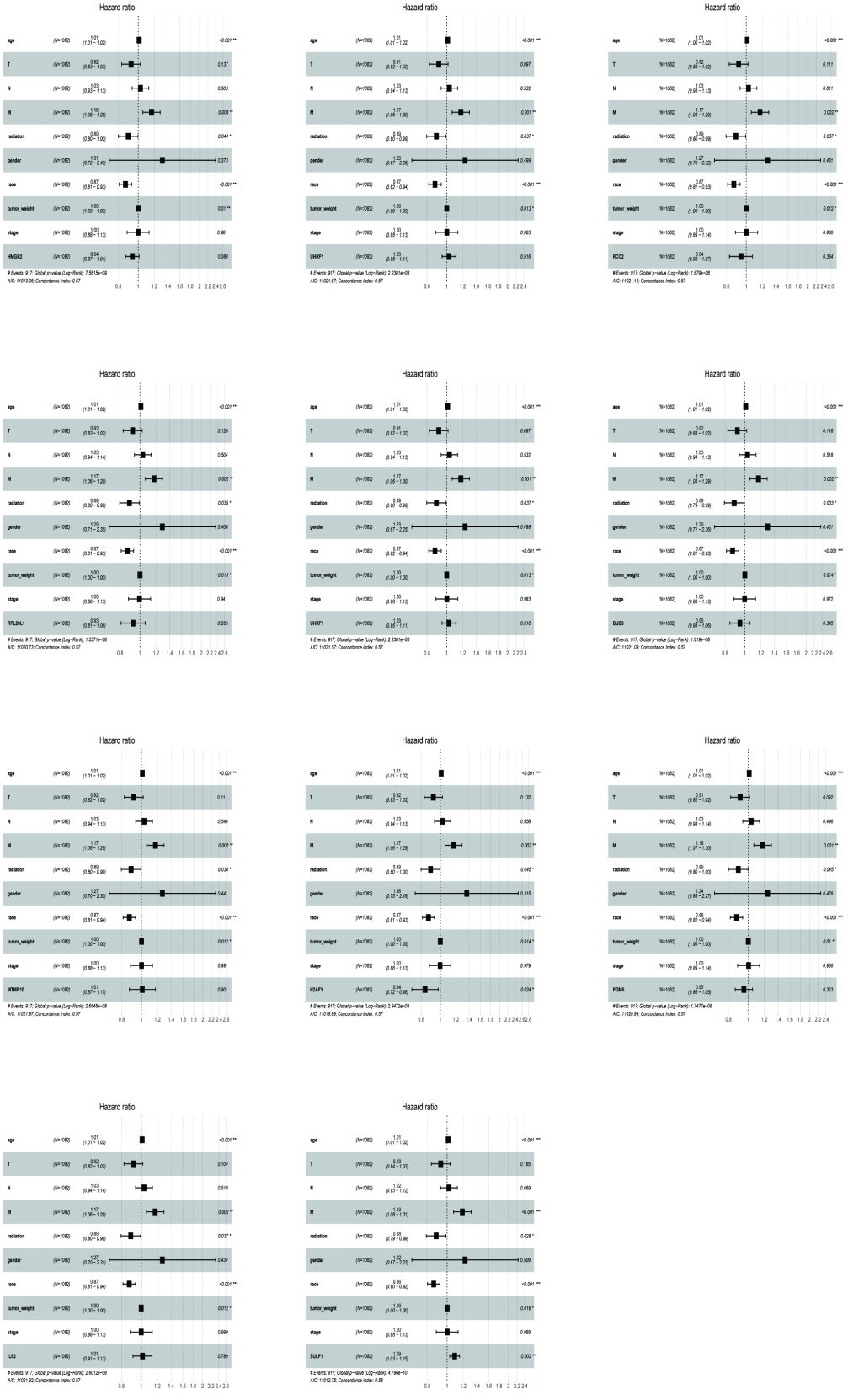

Supplementary Figure S3: Forest plot showed the detailed correlation between 11 differentially genes expression and clinical traits of breast cancer.

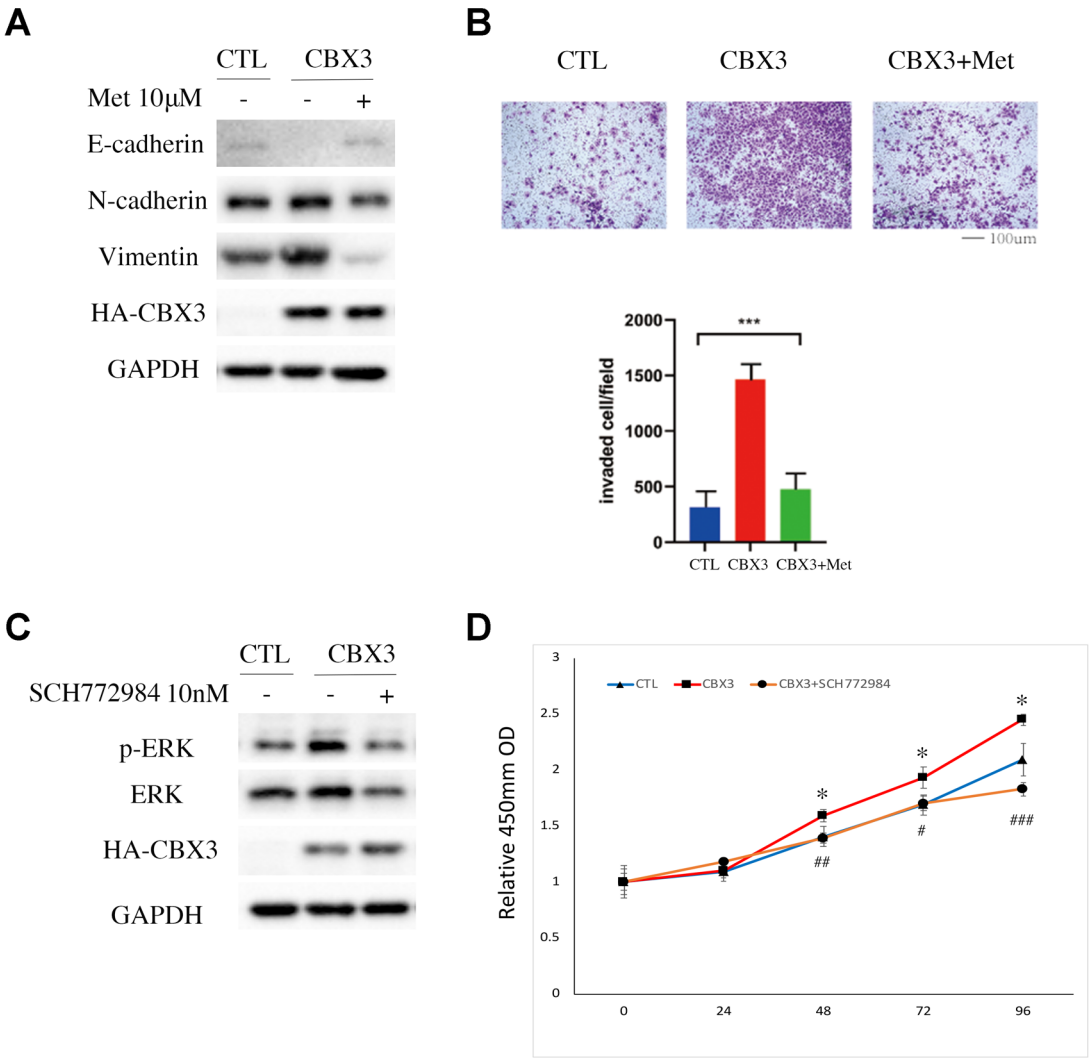

Supplementary Figure S4: CBX3 promoted breast cancer cells migration, invasion and progression via regulating EMT-related proteins and ERK1/2 expression. A) Metformin inhibited CBX3 induced Vimentin, N-cadherin expression. B) Treatment of metformin inhibited cell invasion ability. C) SCH772984 inhibited CBX3 induced ERK1/2 phosphorylation. D) SCH772984 treatment inhibited cell proliferation in CBX3 overexpressed cell.